Cureus Journal of Engineering

Open Access Original Article

Growth and Morphology of Zinc Oxide Thin Films: A Comparative Analysis of Solution-Based Deposition Methods

Received 09/03/2025
Review began 09/17/2025
Review ended 11/09/2025
Published 11/27/2025

DOI:
https://doi.org/10.7759/s44388-025-10030-w

Anupriya S [1] , NandhiniDevi Ganesan [1]

1. Department of Biotechnology, Centre for Food Technology, Anna University, Chennai, IND

Corresponding author: NandhiniDevi Ganesan, projectsagnlabs@gmail.com

Abstract

Zinc oxide (ZnO) has emerged as a promising material for applications in photocatalysis, energy devices, gas sensors, healthcare, and environmental technologies due to its unique physicochemical properties. The performance of ZnO thin films is strongly dependent on the fabrication technique, which governs morphology, surface reactivity, and functional characteristics. This comparative study highlights three solution-based deposition techniques, namely electrospinning, drop-casting, and spin-coating, for the ZnO thin film preparation, followed by hydrothermal treatment to improve crystallinity. Optimized precursor concentrations of 50 mg/mL polyvinyl alcohol and 100 mg/mL $Zn(Ac)_2$ were used for electrospinning, while drop-casting enabled the study of varying hydrothermal conditions. Surface morphology and topography were analyzed using scanning electron microscopy and optical profilometry. Results revealed that spin-coating at 4000 rpm produced highly uniform, thin films with flower-like nanostructures, reduced roughness, and controlled thickness. In contrast, drop-casting resulted in elongated nanorod assemblies with non-uniform distribution, while electrospinning generated disordered, fibrous morphologies with significant irregularities. Fourier-transform infrared spectroscopy confirmed ZnO growth. Overall, spin-coating demonstrated superior control over film morphology and quality, establishing it as the most effective deposition method for ZnO thin films in sensor fabrication.

Categories: Materials Engineering, Polymer Science and Engineering, Nanotechnology
Keywords: zinc oxide films, electrospinning, drop casting, spin coating, hydrothermal treatment

Introduction

Zinc Oxide (ZnO), a widely studied metal oxide, has gained substantial attention due to its intrinsic n-type semiconductor characteristics. Its wide band gap energy (3.3 eV) and high exciton binding energy (60 meV) provide enhanced surface reactivity, making ZnO highly effective for optoelectronic and gas sensing applications, particularly for detecting hydrogen, ammonia, and nitrogen dioxide gases [1]. ZnO possesses a structurally stable framework and a high isoelectric point, which enable superior responsiveness and reliability in biosensing when compared with other metal oxides. Also, a high surface-to-volume ratio further enhances their chemical reactivity and sensing performance, superior to metal oxides like tin, indium, titanium, ferric, and copper oxides. Furthermore, the material exhibits strong ultraviolet (UV) absorption, enabling its integration into UV detectors, lasers, and light-emitting diodes [2]. Beyond electronics, ZnO demonstrates exceptional versatility across solar cells, touch screens, piezoelectric devices, and biomedical systems, with nanoparticles proven to be biocompatible with human cells [3]. It can be synthesized at relatively low temperatures with controlled growth, making it advantageous for diverse structural and functional applications. The resulting nanostructures are chemically and thermally stable under diverse conditions, which is crucial for structural, physical, and functional performance [4]. Moreover, ZnO nanostructures are also known for their morphological diversity, forming nanorods, nanowires, nanosheets, and nanoflowers, with each morphology imparting unique physicochemical and device-specific properties [5]. A wide range of fabrication strategies has been reported for ZnO thin films, including sol-gel processing, hydrothermal synthesis, sputtering, pulsed laser deposition, and chemical or physical vapor deposition [6]. Nanoparticles can be produced by physical (laser ablation, sputtering, thermal treatment, electrodeposition), chemical (sol-gel, precipitation, hydrothermal), or biological (plant extract or microbial-assisted) approaches [7,8]. Among these, hydrothermal synthesis is particularly advantageous, enabling cost-effective, substrate-supported ZnO growth under controlled conditions in a Teflon-lined autoclave [9]. The presence of surface hydroxyl groups and efficient electron-hole generation gives ZnO a strong affinity toward nitrogen-containing polar groups. Structurally, ZnO comprises tetrahedrally coordinated O^{2-} and Zn^{2+} ions, with surfaces exhibiting negatively charged polar planes and positively charged planes, which further influence its sensing behavior [10]. Furthermore, ZnO-based sensors have demonstrated rapid, stable, and sensitive responses for gases such as hydrogen sulfide and ethanol. Common zinc precursors include zinc acetate, zinc chloride, zinc nitrate, and zinc sulfate, typically dissolved in solvents such as deionized water or alcohols (ethanol, methanol, or propanol). Their high stability, rapid response, and sensitivity further make them suitable for diverse applications. In a study, solvothermal synthesis of ZnO nanostructures, $Zn(Ac)_2$, was used as a primary precursor with

How to cite this article
S A, Ganesan N (November 27, 2025) Growth and Morphology of Zinc Oxide Thin Films: A Comparative Analysis of Solution-Based Deposition Methods. Cureus J Eng 2 : es44388-025-10030-w. DOI https://doi.org/10.7759/s44388-025-10030-w

different alcohols like butanol, hexanol, octanol, and decanol as solvent media. This demonstrates that synthesis conditions with higher temperature and concentration enhanced the crystal growth with longer lengths of nanorods, while the aspect ratio was affected by the dissolving medium [6]. A study reported the growth of ZnO nanoparticles via a sol-gel route using ethanolic zinc acetate and lithium hydroxide as precursors. The synthesis process was highly sensitive to parameters such as temperature, water content, and precursor concentration. Stating that a minimal amount of water was essential to initiate nucleation, whereas excess water inhibited ZnO formation [7]. In another study, a comparison was made with aqueous $Zn(Ac)_2$ with ammonia and zinc nitrate with 1,3-hexamethylenetetramine. Both formed hexagonal rod-like structures through the formation of layered basic zinc salts as intermediates, achieved through different pathways. This highlights the fact that the choice of precursor and pH play a decisive role in the morphology of ZnO nanostructures [8]. Doping plays an important role in tailoring ZnO functional attributes. Group 13 elements like gallium and indium ions enhance n-type conductivity when doped with ZnO [9]. A related study shows that trivalent dopants like chromium and yttrium co-doped ZnO enable dielectric modulation [10]. Monovalent dopants like lithium, sodium, and potassium reduce oxygen vacancies, thereby improving optical quality [11]. Divalent ions like magnesium and cadmium alter structural and optical properties and are effective in near UV and blue optoelectronics [12]. So, there is an impending necessity to optimize the ZnO deposition techniques, stating the importance of ZnO in versatile applications. The growth requires optimization with the reaction parameters, including precursor type, temperature, reaction time, and solution concentration, which significantly influence the final nanostructure. In this study, three solution-based deposition methods, namely electrospinning, drop-casting, and spin-coating, are investigated for ZnO thin film fabrication. These methods employ non-toxic, cost-effective, and abundantly available precursors, making them favorable for scalable production [13]. To improve film quality and crystallinity, post-deposition hydrothermal treatment was applied under controlled conditions. Since the functional performance of ZnO is strongly influenced by its structural properties, this work systematically evaluates the selected deposition techniques to assess their suitability for different application requirements, highlighting distinct advantages in terms of scalability, film morphology, and processing conditions.

Materials And Methods

Sample preparation

All chemicals used in this study were of analytical grade and used without any further purification. The primary precursors included Zinc Acetate Dihydrate [$Zn(Ac)_2$], polyvinyl alcohol (PVA) and the dissolving medium is deionized water [14,15]. Glass substrates served as the deposition medium. A homogeneous solution was obtained under mild heating, with continuous stirring at 800 rpm for 24 h in a magnetic stirrer. The deposition techniques, namely electrospinning, drop-casting, and spin-coating, are discussed below.

Electrospinning

To optimize the electrospinning process, the materials were uniformly dispersed in deionized water (D.D. H_2O), and multiple trials were carried out to determine suitable precursor concentrations. PVA solutions were prepared at 50, 100, 150, and 200 mg/ml and electrospun individually. For composite formulations, PVA and $Zn(Ac)_2$ were tested in the following combinations (mg/ml): (50,100), (100,100), (150,100), and (200,100). All precursor solutions were stirred for 1 h under mild heating to ensure uniform dispersion [10]. The prepared solutions were deposited onto a substrate supported by aluminum foil and dried under ambient conditions. Electrospinning was performed using the ESPIN-NANO system with an applied voltage of 20 kV, a flow rate of 1 ml/h, and a 5 ml syringe as the feed reservoir [16]. Rheology of the precursor solution was carried out before electrospinning. The viscosity of the precursor solutions was measured using a Brookfield rotational viscometer at a controlled temperature. Surface tension measurements were performed using a drop volume tensiometer. The electrical conductivity of the solutions was determined using a portable multiparameter conductivity meter (Hanna Instruments, Model HI98195), following instrument calibration before measurement. Hydrothermal treatment was carried out only on the best electrospun sample.

Drop-casting

For the drop-casting method, a precursor solution of $Zn(Ac)_2$ and PVA in deionized water (50 and 100 mg/mL, respectively) was prepared by stirring at 700 rpm under mild heating. The solution was then drop-cast onto a glass substrate and annealed at 70°C until a uniform thin film was obtained. The coated substrate was subsequently subjected to hydrothermal treatment in a Teflon-lined stainless-steel autoclave containing the same precursor solution. Different hydrothermal conditions were explored: (i) 90°C for 4 h, (ii) 110°C for 4 h, (iii) 130°C for 4 h, (iv) 150°C for 3 h, and (v) 85°C for 17 h. Following treatment, all substrates were dried at room temperature [17].

Spin-coating

In the spin-coating method, a 100 µl aliquot of the precursor solution, obtained by mixing for uniform dispersion with mild heat ($Zn(Ac)_2$:PVA-50 mg/ml and 100 mg/ml), was coated using an HDLMARC Spin Coater (Model: HO-TH-05). Four samples were spin-coated at 1500, 2000, 3000, and 4500 revolutions per minute (rpm) each for 30 s with acceleration at 150 rpm/s [18].

The films from each deposition technique were subjected to detailed characterization. Scanning Electron Microscopy (SEM) was used to investigate the surface morphology and confirm the formation of hierarchical ZnO structures. The topography and thickness of the spin-coated samples were measured using profilometry in Vision 4 software, BRUKER Contour GT Optical Profilometer. Fourier Transform Infrared (FTIR) Spectroscopy was employed using Shimadzu IRTracer-100 with CMAT to identify functional groups and verify interactions between the metal oxide framework and the polymeric matrix. X-ray diffraction (XRD) analysis was carried out using a Thermo Scientific X-ray Diffractometer to identify and analyze the crystalline nature of the material.

Results And Discussion

Deposition techniques

The electrospun solution at a concentration of 50 mg/ml PVA and 100 mg/ml $Zn(Ac)_2$ had optimal extrusion from the syringe as shown in Table *1* and was further grown hydrothermally at 135℃ for 8 h [19]. This optimized precursor concentration was subsequently employed for drop-casting and spin-coating onto the substrates.

S. No	Composition (mg/ml)	Viscosity (Pa·s)	Conductivity (µS/cm)	Surface Tension (mN/m)	Observations
1	PVA 50	29-35	58.9 ± 0.5	33.5 ± 0.5	Too dilute, extruded as droplets
2	PVA 100	30-46	120 ± 2.5	36.1 ± 2.5	Extruded in watery form, unstable filaments
3	PVA 150	32-79	171 ± 0.5	37.6 ± 1.7	Very viscous, poor extrusion
4	PVA 200	100-180	253 ± 0.7	40.2 ± 0.5	Highly viscous, not suitable for extrusion
5	PVA 50 + $Zn(Ac)_2$ 100	110-170	9440 ± 2.5	47.5 ± 1.7	Optimal: Smooth extrusion with initial filament formation
6	PVA 100 + $Zn(Ac)_2$ 100	70-90	8300 ± 4.0	48.3 ± 0.6	Discontinuous film formation obtained
7	PVA 150 + $Zn(Ac)_2$ 100	180-230	6800 ± 1.6	49.2 ± 1.3	Excess viscosity, extrusion hindered
8	PVA 200 + $Zn(Ac)_2$ 100	150-190	5000 ± 1.9	51 ± 0.75	Highly viscous, not extrudable
9	PVA 100 + $Zn(Ac)_2$ 100	40-56	300 ± 4.0	22.4 ± 1.5	Partial improvement, slight filaments, but mostly watery

TABLE 1: Extrusion of solution through electrospinning

Optical profilometry

This process facilitated uniform spreading and strong adhesion of the ZnO thin films onto the substrate. The spin-coated samples were subsequently examined in detail to evaluate surface roughness and topography using both two-dimensional (2D) and three-dimensional (3D) analyses. Figure *1*, Figure *2*, Figure *3*, and Figure *4* present the 3D images of spin-coated films obtained at 1500, 2000, 3000, and 4000 rpm, respectively. The corresponding 2D surface roughness parameters of the films spin-coated at the same speeds for 30 s are summarized in Table *2* as Samples 1-4. The tabulated values include root mean square roughness (Rq), average roughness (Ra), total roughness (Rt), maximum peak height (Rp), and maximum valley depth (Rv).

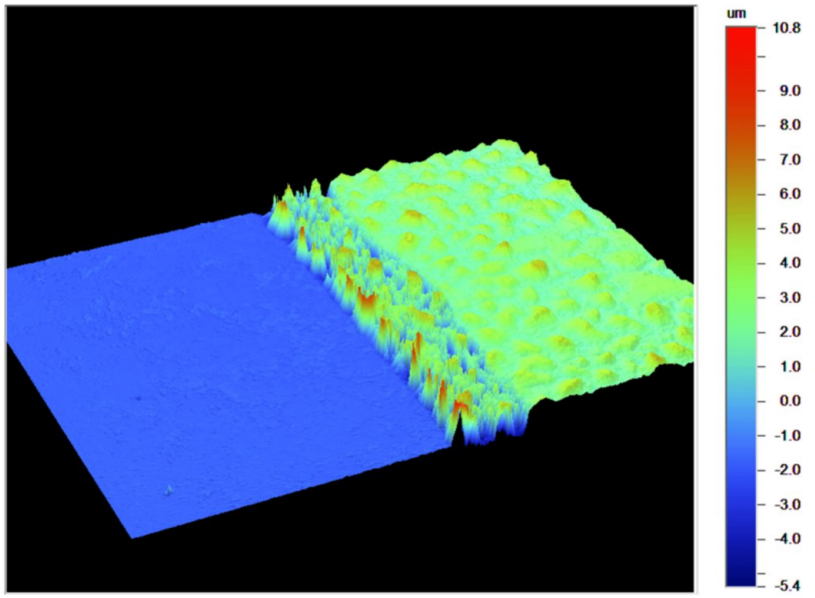

FIGURE 1: Representation of optical profilometry of sample at 1500 rpm

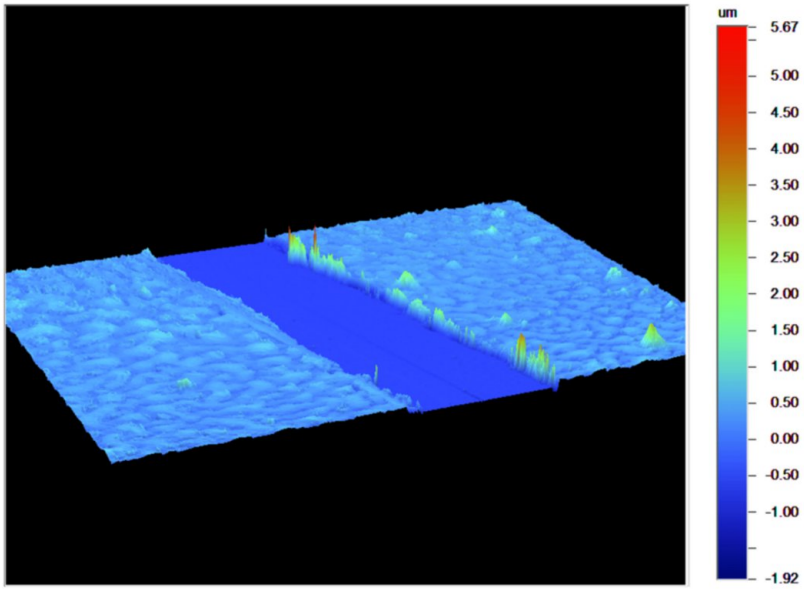

FIGURE 2: Representation of optical profilometry of sample at 2000 rpm

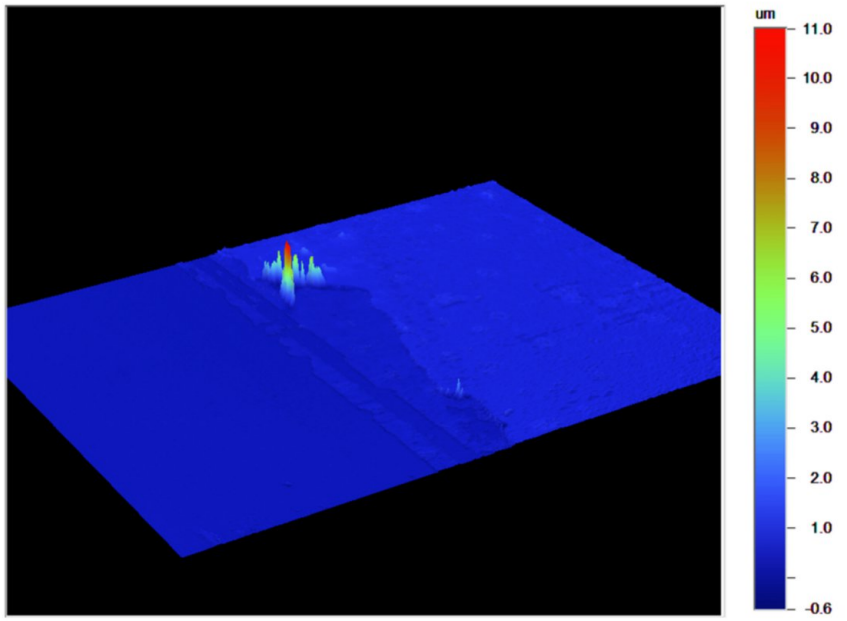

FIGURE 3: Representation of optical profilometry of sample at 3000 rpm

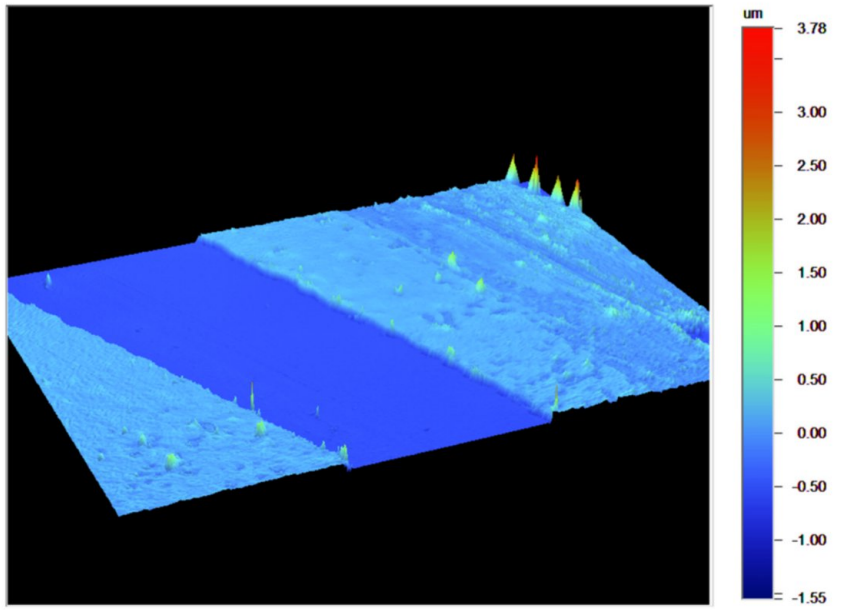

FIGURE 4: Representation of optical profilometry of sample at 4000 rpm

Analysis of Table *2* indicates that surface roughness in the X-profile decreases progressively with increasing spin speed. At lower rpm (e.g., 1500 rpm), the films exhibit higher roughness, associated with greater thickness and less uniformity. Conversely, at higher rpm (e.g., 4000 rpm), smoother and more uniform films are obtained due to the formation of thinner layers. The suitability of different thicknesses depends on the intended application of ZnO films. For instance, in gas-sensing applications, films spin-coated at 4000 rpm for 30 s are particularly advantageous, as their uniformity, reduced thickness result in lower resistance and improved conductivity.

Spin-coating affects the film thickness, uniformity, and surface morphology. In the current system, the

precursor solution of PVA and $Zn(Ac)_2$, at concentrations of 50 and 100 mg/ml in distilled water, spreads across the substrate under centrifugal force. Consequently, the spin speed and the volume of solution dispensed directly influence the final film thickness. The glass substrate, being flat and with high surface energy, encourages rapid wetting of the liquid precursor and even spreading of the solution during rotation. As the spin speed increases, the outward radial flow and solvent evaporation rate are boosted, resulting in a thinner film. Thinner films show fewer vertical height fluctuations (Rp), meaning higher spin speeds generally produce smoother surfaces, as reflected in lower average roughness (Ra) and root-mean-square roughness (Rq), due to better leveling before solidification.

Sample	Profile	Rq (µm)	Ra (µm)	Rt (µm)	Rp (µm)	Rv (µm)
1	X	2.36	2.28	9.06	4.55	4.52
	Y	0.72	0.59	3.06	4.57	1.51
2	X	0.61	0.47	4.04	3.00	-0.94
	Y	0.27	0.23	1.69	1.17	-0.52
3	X	0.41	0.34	2.03	1.65	-0.72
	Y	0.44	0.40	1.80	1.01	-0.79
4	X	0.29	0.28	1.09	0.37	-0.37
	Y	0.10	0.08	0.83	0.43	-0.41

TABLE 2: Surface roughness and topographical parameters of spin-coated ZnO films

Sample 1-1500 rpm; 2-2000 rpm; 3-3000 rpm; 4-4000 rpm

Scanning electron microscopy

The SEM analysis highlights the hierarchical growth of Zinc Oxide (ZnO) nanostructures, which is pivotal for enhancing charge transport and facilitating gas adsorption. The glass substrate was gold sputtered at 30 mA to a thickness of 10 nm prior to taking the SEM. The morphological variations observed across electrospinning, drop-casting, and spin-coating demonstrate the strong influence of deposition techniques on the structural and functional properties of ZnO films. Figure *5* to Figure *10* show images of the distinct morphologies obtained by electrospun, drop-casted, and spin-coated samples.

Figure *5* shows the sample prepared by electrospinning, exhibiting a highly irregular, fibrous morphology. The structure appears largely amorphous with ZnO dispersed within the polymeric matrix as rod-shaped non-uniform crystallites with mixed spherical and irregular growth. The non-uniform distribution is attributed to rapid solvent evaporation during the electrospinning process. While crystallinity is poor, such disordered morphologies can be beneficial for catalytic degradation applications due to the higher defect density and active surface sites.

Figure *6*, Figure *7*, Figure *8*, and Figure *9* correspond to the drop-cast films of samples (i, ii, iii, and iv), respectively. Figure *6* signifies an irregular, porous, and non-uniform structural arrangement. Figure *7* presents well-defined, elongated nanorods arranged in a relatively uniform pattern, which is favorable for gas sensing applications owing to the high aspect ratio and active surface exposure [20,21]. In contrast, Figure *8* displays nanosheets with sharp, spike-like edges and enhanced crystallinity, making them suitable for optoelectronic and photocatalytic applications, where charge transfer is critical [22,23]. In Figure *9*, the ZnO films exhibit a flower-like arrangement with high surface reactivity and excellent electron mobility, rendering them suitable for gas sensing. Thus, the temperature of the hydrothermal treatment plays a major role in the morphology of the structures.

The morphology of the good spin-coated sample from the profilometry study, showcased in Figure *10*, evolves into densely packed flower-like structures, providing a larger surface-to-volume ratio and improved electron connectivity. These hierarchical nanostructures enhance surface-active sites, which facilitate charge transfer, and are highly advantageous for UV detectors and energy devices [24]. Controlled nucleation achieved through optimized hydrothermal treatment after spin coating enhances the crystallinity and functional stability of ZnO thin films. Compared to the other two deposition techniques, spin coating produces a more uniform morphology, thereby improving the overall functional performance of the substrate.

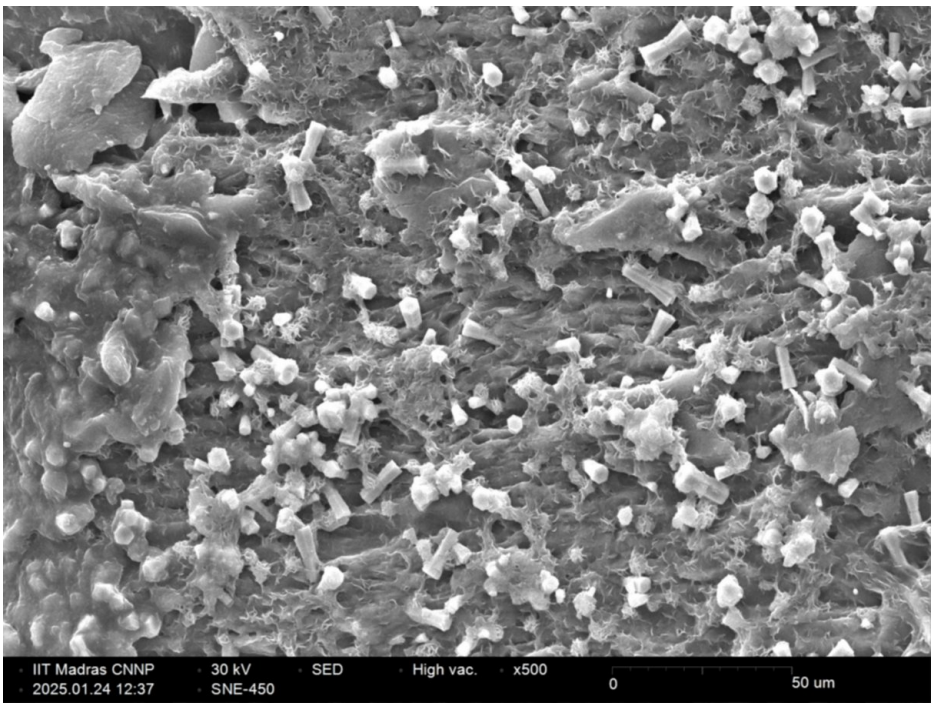

FIGURE 5: Morphology of ZnO obtained through electrospinning

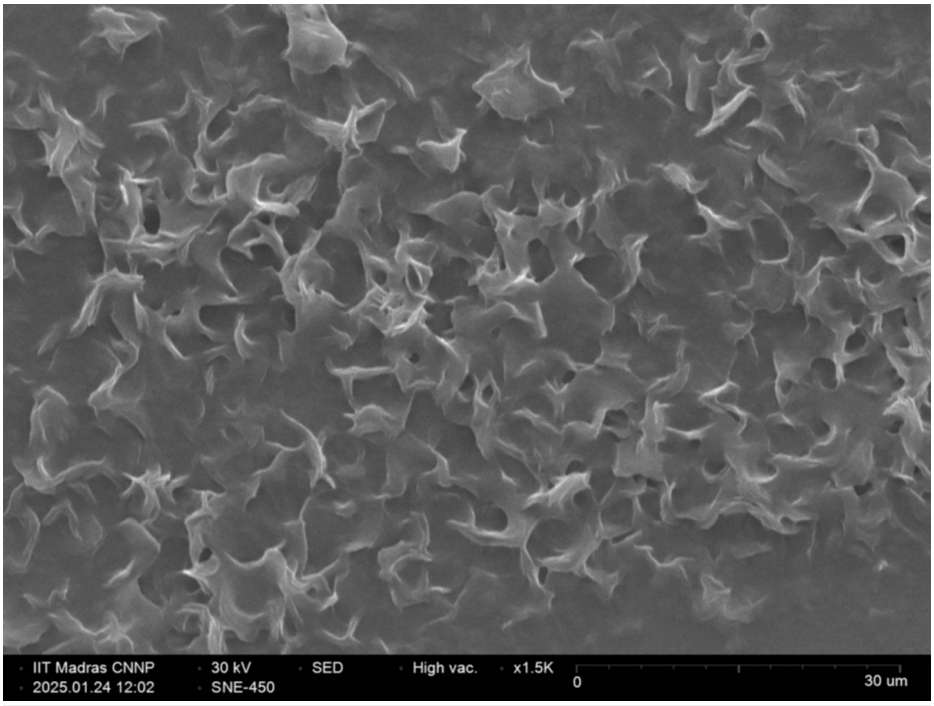

FIGURE 6: Morphology of ZnO obtained through drop-casting-sample (i)

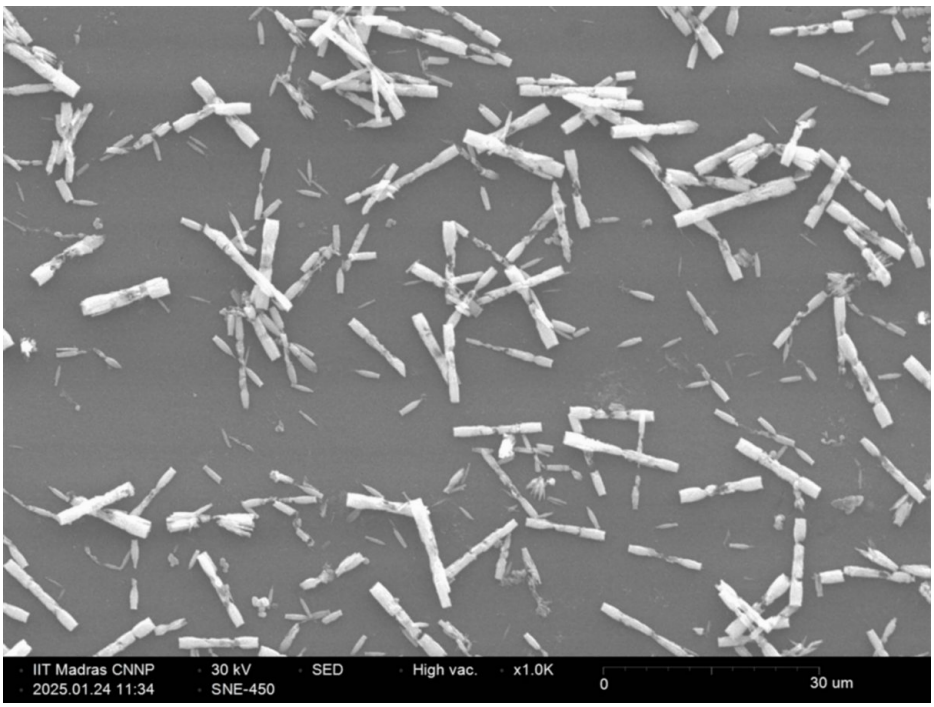

FIGURE 7: Morphology of ZnO obtained through drop-casting-sample (ii)

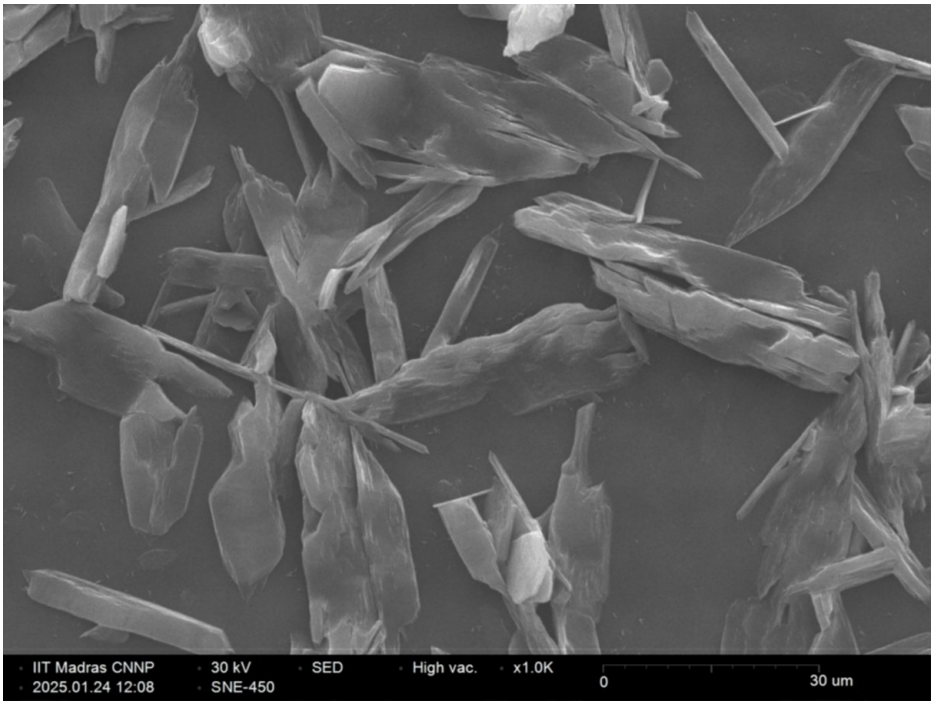

FIGURE 8: Morphology of ZnO obtained through drop-casting-sample (iii)

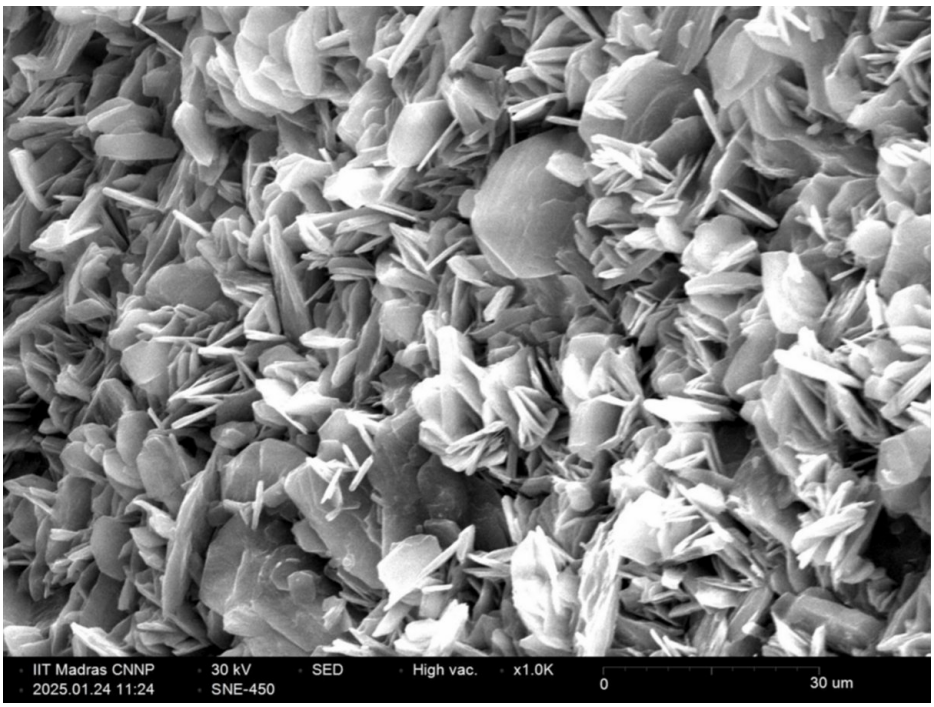

FIGURE 9: Morphology of ZnO obtained through drop-casting-sample (iv)

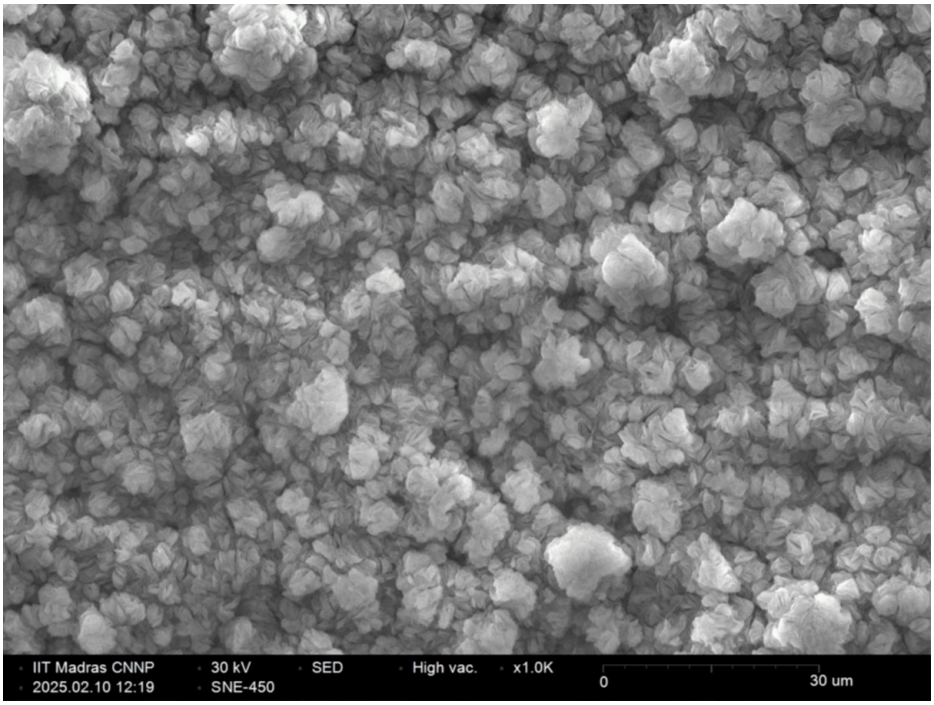

FIGURE 10: Morphology of ZnO obtained through spin coating

Fourier Transform Infrared Spectroscopy

FTIR spectroscopy was carried out in the range of 400-4000 cm^{-1} to identify the functional groups present in the sensitive film. The spectra were recorded for spin-coated unannealed samples prepared at 1500 rpm, and the results confirmed the formation of ZnO through characteristic chemical interactions between the precursor components. As shown in Figure *11*, the spectrum plots wavenumber (cm^{-1}) against % transmittance. A prominent absorption band observed in the region of 678-763 cm^{-1} corresponds to Zn-O stretching vibrations, which lies in the fingerprint region and confirms the successful growth of ZnO

nanoparticles [14,19,20]. Additional peaks between 1020 and 3325 cm^{-1} indicate the presence of residual functional groups. The peak at 1022 cm^{-1} is attributed to C-O-C stretching of the PVA backbone, while the bands at 1392 and 1537 cm^{-1} correspond to the symmetric and asymmetric stretching of COO^- groups, respectively, arising from acetate residues of the zinc acetate precursor. A broad band around 3325 cm^{-1} corresponds to O-H stretching vibrations, further supported by the extended broad absorption observed between 3219 and 3921 cm^{-1}, which is the characteristic of hydroxyl groups. These observations suggest that, along with ZnO formation, acetate and PVA residues remain as surface impurities on the ZnO nanostructures.

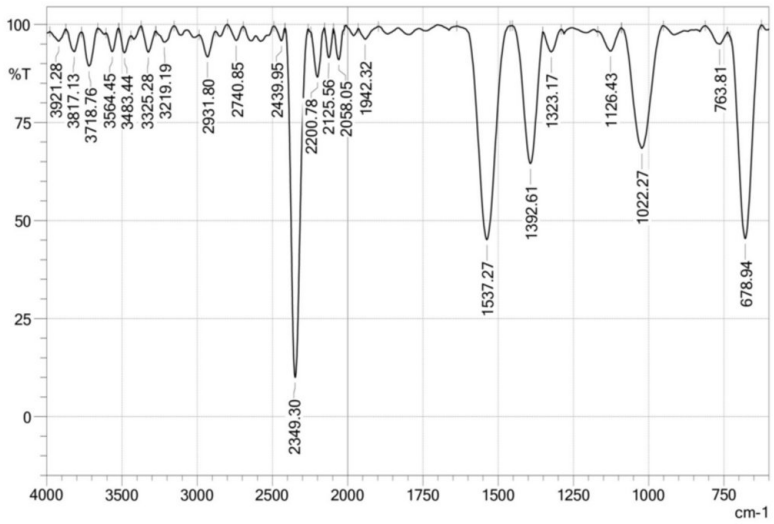

FIGURE 11: FTIR characteristic spectrum of the ZnO

FTIR, Fourier Transform Infrared

X-ray diffraction

The XRD pattern of the synthesized ZnO in Figure *12* shows diffraction peaks comparable with the standard wurtzite ZnO phase (JCPDS No. 03-065-2880). The prominent reflection at 2θ ≈ 38.37°, corresponding to the (101) plane, exhibits a calculated interplanar spacing of 2.34 Å, while the high-angle peak at 2θ ≈ 88.90° corresponds to a d-spacing of 1.10 Å, confirming the crystalline lattice of ZnO. The absence of additional diffraction peaks indicates that the sample is phase-pure and possesses a well-defined crystalline structure.

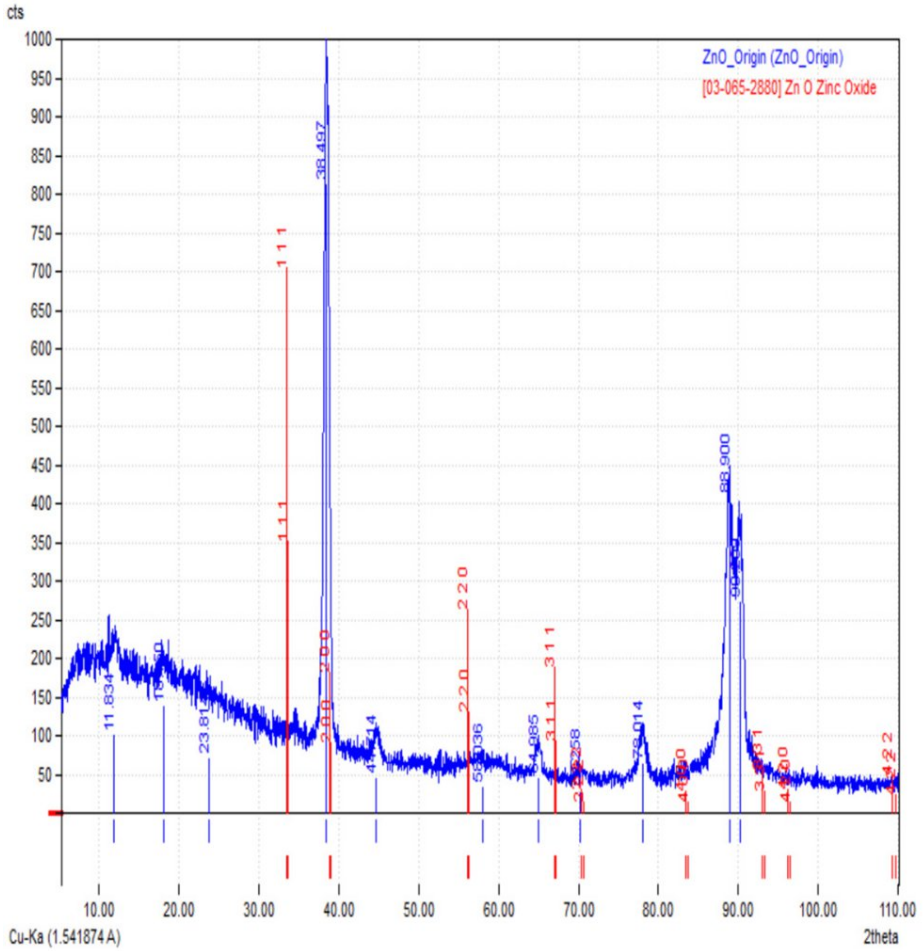

FIGURE 12: XRD pattern of the ZnO spin-coated sample. The red line denotes the standard peaks given from the JCPDS card No 03-065-2880

XRD, X-ray diffraction

Discussion

The morphology of ZnO thin films was strongly influenced by the deposition technique, which governs the structural arrangement and functional suitability. Spin-coating with hydrothermal treatment produced the most uniform and hierarchically ordered nanostructures, making them ideal for device applications. In contrast, drop-casting led to anisotropic growth with randomly arranged structures, while electrospinning yielded amorphous fibrous morphologies with limited utility. Hydrothermal treatment was crucial, as controlled nucleation enhanced crystallinity and film stability. FTIR further confirmed ZnO formation through Zn-O stretching bands and revealed residual organics from precursors that assisted oxide growth. Overall, hydrothermal processing decisively improved ZnO growth and functional performance. Besides, XRD results also prove the crystalline nature of the grown ZnO.

Conclusions

This study presents a comparative analysis of various deposition techniques and their influence on the resulting ZnO nanostructures. In the electrospinning method, the optimized precursor concentrations were determined to be 50 mg/mL for PVA and 100 mg/mL for $Zn(Ac)_2$, ensuring better extrusion properties. For drop-casting, different hydrothermal growth conditions were explored by varying reaction time and temperature. SEM analysis of these films revealed non-uniform nanostructure distribution, which prompted further optimization through spin-coating. Spin-coating was performed at rotational speeds of 1000, 2000, 3000, and 4000 rpm, and film roughness was subsequently quantified using profilometry. Films prepared at 4000 rpm exhibited the lowest thickness and superior surface quality. SEM characterization confirmed a uniform surface morphology and homogeneous film distribution in the spin-coated samples, which was further enhanced after hydrothermal treatment at elevated temperatures and extended durations, optimized via the drop-casting trials. The hydrothermal process was found to significantly improve crystallinity, thereby enhancing charge transport pathways and ensuring long-term

operational stability of the films. In contrast, deposition methods such as drop-casting and electrospinning produced films with non-uniform thickness, higher roughness, and prominent surface defects. Collectively, the results establish spin-coating combined with hydrothermal treatment as the most effective deposition strategy, offering precise control over film thickness, smoothness, and structural integrity-key parameters for high-performance sensor applications. FTIR and XRD confirm the growth of ZnO with high purity and a crystalline nature.

Future work should focus on optimizing process parameters and strategically incorporating dopants to tailor ZnO films for advanced applications in next-generation gas and biosensors. Moreover, efforts toward developing scalable and cost-effective deposition strategies will be crucial to enable industrial feasibility and widespread adoption.

Additional Information

Author Contributions

All authors have reviewed the final version to be published and agreed to be accountable for all aspects of the work.

Concept and design: Anupriya S, NandhiniDevi Ganesan

Acquisition, analysis, or interpretation of data: Anupriya S, NandhiniDevi Ganesan

Drafting of the manuscript: Anupriya S, NandhiniDevi Ganesan

Critical review of the manuscript for important intellectual content: Anupriya S, NandhiniDevi Ganesan

Supervision: NandhiniDevi Ganesan

Disclosures

Human subjects: All authors have confirmed that this study did not involve human participants or tissue. **Animal subjects:** All authors have confirmed that this study did not involve animal subjects or tissue. **Conflicts of interest:** In compliance with the ICMJE uniform disclosure form, all authors declare the following: **Payment/services info:** This work was supported by the Anusandhan National Research Foundation (ANRF), Government of India. **Financial relationships:** All authors have declared that they have no financial relationships at present or within the previous three years with any organizations that might have an interest in the submitted work. **Other relationships:** All authors have declared that there are no other relationships or activities that could appear to have influenced the submitted work.

Acknowledgements

We express sincere gratitude to the Indian Nanoelectronics Users Programme-Idea to Innovation at IIT Madras (INUP-i2i, IITM), funded by the Ministry of Electronics and Information Technology (MeitY), for granting access to fabrication and characterization facilities at the Centre for NEMS and Nanophotonics (CNNP), IIT Madras. "This article was previously presented at the International Conference on Advanced Materials & Characterization 2025 (ICAMC 2025) at Sathyabama Institute of Science and Technology (SIST) - on 11th–13th August 2025."

References

1. Raja K, Ramesh PS, Geetha D: Structural, FTIR and photoluminescence studies of Fe doped ZnO nanopowder by co-precipitation method. Spectrochimica Acta Part A: Molecular and Biomolecular Spectroscopy. 2014, 131:183-88. 10.1016/j.saa.2014.03.047
2. Achehboune M: Microstructural, FTIR and Raman spectroscopic study of Rare earth doped ZnO nanostructures. Materials Today: Proceedings. 2021, 53:319-23. 10.1016/j.matpr.2021.04.144
3. Gharagozlou M, Naghibi S: Sensitization of ZnO nanoparticle by vitamin B12: Investigation of microstructure, FTIR and optical properties. Materials Research Bulletin. 2016, 84:71-78. 10.1016/j.materresbull.2016.07.029
4. Shkir M: Development of highly sensitive Al, Ga, and In-doped ZnO films by the drop casting method for NH3 gas sensing. New Journal of Chemistry. 2023, 47:4880-887. 10.1039/d2nj05323c
5. Wattigney WA, Rice N, Cooper DL, Drew JM, Orr MF: State programs to reduce uncontrolled ammonia releases and associated injury using the hazardous substances emergency events surveillance system. Journal of Occupational and Environmental Medicine. 2009, 51:356-63. 10.1097/JOM.0b013e318197368e
6. Tonto P, Mekasuwandumrong O, Phatanasri S, Pavarajarn V, Praserthdam P: Preparation of ZnO nanorod by solvothermal reaction of zinc acetate in various alcohols. Ceramics International. 2008, 34:57-62. 10.1016/j.ceramint.2006.08.003
7. Meulenkamp EA: Synthesis and growth of ZnO nanoparticles. The Journal of Physical Chemistry B. 1998, 102:5566-572.
8. Liang MK, Limo MJ, Sola-Rabada A, Roe MJ, Perry CC: New insights into the mechanism of zno formation from

aqueous solutions of zinc acetate and zinc nitrate. Chemistry of Materials. 2014, 26:4119-129. 10.1021/cm501096p

9. Seid ET, Dejene FB: Gallium and indium co-doping effects on structural, optical and luminescence properties of ZnO nanostructures. Materials Today Communications. 2021, 27:102330. 10.1016/j.mtcomm.2021.102330
10. Debnath T, Chakraborty T, Bandyopadhyay A, et al.: Site selective response of cationic dopants in ZnO nanomaterials: Optical, dielectric and magnetic behaviors. Materials Chemistry and Physics. 2023, 296:127284. 10.1016/j.matchemphys.2022.127284
11. Yousefi R, Zak AK, Jamali-Sheini F: The effect of group-I elements on the structural and optical properties of ZnO nanoparticles. Ceramics International. 2013, 39:1371-377. 10.1016/j.ceramint.2012.07.076
12. Kalu O, Duarte Moller JA, Reyes Rojas A: Structural and optical properties of cadmium magnesium zinc oxide (CdMgZnO) nanoparticles synthesized by sol-gel method. Physics Letters A. 2019, 383:1037-46. 10.1016/j.physleta.2018.11.052
13. Mandal AK: Current research on Zinc Oxide nanoparticles: Synthesis, characterization, and biomedical applications. Nanomaterials. 2022, 12:3066. 10.3390/nano12173066
14. Oliveira VHB: Electrospun fibers of poly (vinyl alcohol): zinc acetate (PVA:AcZn) and further ZnO production: evaluation of PVA:AcZn ratio and annealing temperature effects on ZnO structure. Journal of Nanoparticle Research. 2020, 22:322. 10.1007/s11051-020-05048-6
15. Abdulhussain R, Adebisi A, Conway BR, Asare-Addo K: Electrospun nanofibers: Exploring process parameters, polymer selection, and recent applications in pharmaceuticals and drug delivery. Journal of Drug Delivery Science and Technology. 2023, 90:105156. 10.1016/j.jddst.2023.105156
16. Abed SM, Mohammad SM, Hassan Z, Muhammad A, Rajamanickam S, Ali K: Comparative study of UV-ZnO NRs photodetectors based on seeded porous silicon by RF-sputtering and drop-casting methods. Journal of Materials Science: Materials in Electronics . 2022, 33:26322-6342. 10.1007/s10854-022-09315-1
17. Denchitcharoen S, Siriphongsapak N, Limsuwan P: Growth of ZnO nanosheets by hydrothermal method on ZnO seed layer coated by spin-coating technique. Materials Today: Proceedings. 2017, 4:6146-152. 10.1016/j.matpr.2017.06.108
18. Li Y, Jiao M, Yang M: In-situ grown nanostructured ZnO via a green approach and gas sensing properties of polypyrrole/ZnO nanohybrids. Sensors and Actuators B: Chemical. 2017, 238:596-604. 10.1016/j.snb.2016.07.089
19. Gao T, Wang TH: Synthesis and properties of multipod-shaped ZnO nanorods for gas-sensor applications. Applied Physics A. 2005, 80:1451-454. 10.1007/s00339-004-3075-2
20. Tiwary P, Chakrabarty N, Chakraborty AK, Mahapatra R: Flower-like ZnO nanostructures as gas sensor. Materials Today: Proceedings. 2019, 11:875-78. 10.1016/j.matpr.2019.03.059
21. Patel SS, Sengunthar P, Thankachen N, Joshi US: Optoelectronic properties of optimally grown ZnO nanorods. Journal of Materials Science: Materials in Electronics. 2022, 33:6432-445.
22. Zhang X, Qin J, Xue Y, Yu P, Zhang B, Wang L, Liu R: Effect of aspect ratio and surface defects on the photocatalytic activity of ZnO nanorods. Scientific Reports. 2014, 4:4596. 10.1038/srep04596
23. Pallavolu MR, Maddaka R, Viswanath SK, Banerjee AN, Kim MD, Joo SW: High-responsivity self-powered UV photodetector performance of pristine and V-doped ZnO nano-flowers. Optics & Laser Technology. 2023, 157:108776. 10.1016/j.optlastec.2022.108776
24. Kumar RD, Kumar AJ, Balachandran S, et al.: High-performance chrysanthemum flower-like structure of Ni doped ZnO nanoflowers for pseudo-supercapacitors. Journal of Energy Storage. 2023, 72:108441. 10.1016/j.est.2023.108441